

# Improved predictions of the standard model and the detection of new physics in neutron beta decay.

A. García\*, and J.L. García-Luna\*,†<sup>1</sup>

\*Departamento de Física, Centro de Investigación y de Estudios Avanzados del IPN, Apartado Postal 14-740, 07000 México, Distrito Federal, México.

†Departamento de Física, Centro Universitario de Ciencias Exactas e Ingenierías, Universidad de Guadalajara, Blvd. Marcelino García Barragan 1508, C.P. 44840, Guadalajara Jalisco, México.

---

## Abstract

We improve the current predictions of the standard model for neutron beta decay observables and compare them with the currently available ones. Next we study their implications in the possible detection of new physics. We discuss where the limitations are and where further efforts should be directed.

---

**Introduction.** As precision measurements in neutron beta decay ( $n\beta d$ ) have become available, interest in detecting physics beyond the standard model (SM) in this decay has increased steadily[1]. However, the predictions of the SM for  $n\beta d$  observables seem to be severely afflicted by our current inability to calculate the leading form factors ratio  $\lambda = g_1/f_1$  and the Cabibbo-Kobayashi-Maskawa (CKM) matrix element  $V_{ud}$ . It imposes on them two general restrictions, namely, the  $V - A$  structure of the weak vertex and the unitary of the CKM matrix, respectively. Otherwise these two quantities remain as free parameters to be determined from experiment. With current experimental error bars a region in the  $(\lambda, R)$ - plane ( $R$  is the decay rate) can be determined where the SM remains valid at, say, 90% C.L. We shall refer to this region as the standard model region (SMR). Our main purpose in this paper is to reduce this region as much as possible, thereby, improving the predictions of the SM. Next we shall study the usefulness of this improved region in either detecting new physics or imposing more strict bounds on its existence. Finally, we shall discuss how future efforts in this respect should be directed. Another important aspect to discuss is the limitations for the detection of new physics

---

<sup>1</sup> E-mail: jlgarcia@fis.cinvestav.mx

in  $n\beta d$ . As precision measurements improve, the limitations will be come significant enough as to render the detection of new physics in this decay very obscure or even hopeless.

**Procedure.** As we just mentioned agreement of the SM with  $n\beta d$  can occur only in the region of the  $(\lambda, V_{ud})$  plane or equivalently of the  $(\lambda, R)$  plane where both the  $V - A$  and the unitarity restrictions are satisfied, namely the SMR. Disagreement, and along with it the possibility to detect new physics, corresponds to the region in such planes where the restrictions are no longer satisfied. We shall refer to this other region as the new physics region (NPR). we shall proceed determine these two regions.

One can show that up to a precision of  $10^{-4}$  the observables in  $n\beta d$  depend only on two parameters, namely, the (CKM) matrix element  $V_{ud}$  and the ratio  $\lambda$  [2]. All other contributions up to this precision are well determined (through the use of the conserved vector-current hypothesis, model-independent and reliable estimates of model-dependent radiative corrections, etc.). We shall use the angular asymmetry coefficients  $\alpha_e$ ,  $\alpha_{e\nu}$ , and  $\alpha_\nu$  (imposing the  $V - A$  restriction through  $\lambda$ ), the CKM  $V_{us}$  and  $V_{ub}$  matrix elements (imposing the unitarity restriction  $V_{ub} = \sqrt{1 - V_{ud}^2 - V_{us}^2}$ ), and  $R$ . Then we form a  $\chi^2$  function with six terms. The first four terms compare the theoretical expressions of the  $\alpha_e$ ,  $\alpha_{e\nu}$ ,  $\alpha_\nu$  and  $R$  as functions of  $\lambda$  and  $V_{ud}$  with their experimental counterparts, the fifth term compares  $V_{ub}$  of the unitarity square root with its experimental counterpart, and the last term constrains  $V_{us}$  to its experimental value.

The precision measurements in  $n\beta d$  occur in  $R$  and  $\alpha_e$ . The state-of-the-art will allow that their error bars be reduced to about one tenth of their current values [3]. In order to determine the SMR we shall concentrate on these two quantities. We shall keep the other four fixed at their present experimental values [4], namely,  $\alpha_{e\nu} = -0.0766(36)$ ,  $\alpha_\nu = 0.9830(40)$ ,  $V_{ub} = 0.0036(10)$  and  $V_{us} = 0.2196(23)$ . We have folded the theoretical error into the current value of  $R$  to give  $R = 1.12879(110)$  [2]. It is customary to quote the experimental value of  $\lambda$  instead of  $\alpha_e$  and we shall follow this practice, i.e., in  $\chi^2$  we shall replace  $\alpha_e$  by  $\lambda$ . There are at present [5,6,7,8] four precise measurements of  $\lambda$  (all them through  $\alpha_e$ ), namely,  $\lambda_L = 1.2660(40)$ ,  $\lambda_B = 1.2620(50)$ ,  $\lambda_Y = 1.2594(38)$ , and  $\lambda_R = 1.2735(21)$ . This last value is slightly revised in [1]. The first three are statistically compatible and their average is  $\lambda_{LYB} = 1.2624(24)$ . One may quote the average of the four,  $\lambda_{LYBR} = 1.2687(16)$ . However, this average is not statistically consistent and one should really keep  $\lambda_R$  separate from the other three. At any rate the error bars of  $\lambda_{LYB}$  and  $\lambda_R$  are comparable, so one may take a typical  $\sigma_\lambda = 0.0024$ . Because of this situation we shall cover  $5\sigma_\lambda$  to the right and  $3\sigma$  to the left of  $\lambda_{LYB}$ .

For definiteness, we shall work in the  $(\lambda, R)$  plane. Our procedure to determine the SMR is to calculate  $\chi^2$  at points  $(\lambda, R)$  covering the rectangle in this plane with sides  $(1.256, 1.274)$  for  $\lambda$  and  $(1.12549, 1.13209)$  for  $R$ . This latter is the  $\pm 3\sigma_R$  range. The values of  $\lambda$  and  $R$  in the points  $(\lambda, R)$  are used as

the “experimental” central values in the  $\chi^2$  function. For the “experimental” error bars we shall consider three possibilities. First we take  $\sigma_\lambda$  and  $\sigma_R$  at their current values, next we take for them one tenth of those current values, and last we take for them one thousandth of such values.

**Results.** Our numerical results are displayed in Table 1. There we show the 90% and 95% ranges for  $\lambda$  at sample values of  $R$  (which go in steps of one current  $\sigma_R$  up to  $\pm 3\sigma_R$  around its present experimental central value). For each value of  $R$  we give three entries; the upper, middle, and lower ones correspond to current error bars, future one tenth error bars, and, so to speak, “ideal” one thousandth error bars, respectively. All these numbers are easily visualized in Figs. 1-3. The bands within the dotted lines correspond to the 90% SMR in the three cases considered. In each of these figures we have also depicted with I, II, and III the 90%CL ellipses around  $\lambda_{LYB}$ ,  $\lambda_R$  and  $\lambda_{LYBR}$ , respectively. In figures 2 and 3 we also show the 90%CL ellipses corresponding to one tenth of  $\sigma_\lambda$  and  $\sigma_R$  around these three central values and also around a central value previously reported in [9],  $\lambda_W = 1.2657(30)$ . These figures make it very easy to reach several conclusions. The  $\lambda_{LYB}$  and  $\lambda_R$  with their current error bars both fall completely at a 90%CL in the NPR, i.e., each one gives a strong signal for the existence of new physics. This cannot be seen in Fig. 1, but it becomes very clear in Figs. 2 and 3. Of course, since they fall on opposite sides of SMR, the situation is yet undecided. Another conclusion is that the SMR is greatly improved by reducing  $\sigma_R$  and  $\sigma_\lambda$  by one tenth; but, even though there is some improvement, to further reduce  $\sigma_R$  and  $\sigma_\lambda$  does not provide a substantial gain. The reason is that in Fig. 2 The error bars of  $V_{us}$  already dominate. This is clearly seen in Fig. 3, where the width of the SMR is due almost entirely to the  $V_{us}$  error bars.

**The the detection of new physics in  $n\beta d$ .** The ability of  $n\beta d$  to resolve new physics depends on where in the  $(\lambda, R)$  plane the future  $(\lambda_{exp.}, R_{exp.})$  will lie as well as on their future accompanying error bars. One may appreciate this by looking at the values of  $\chi^2$  at points covering the rectangle we are studying. For this purpose we have produced Table 2. In each entry we give two numbers. The upper one uses the current  $\sigma_R$  and  $\sigma_\lambda$ , the lower one uses one tenth of  $\sigma_R$  and  $\sigma_\lambda$ .  $\chi^2$  does not further increases substantially if one uses one thousandth of  $\sigma_R$  and  $\sigma_\lambda$ , but we shall not produce the corresponding numbers in Table 2.  $\chi^2$  may reach impressively high values.

There is another way to appreciate this resolving power. This can be seen in Table 3. We selected the four values of  $\lambda$  marked as I-IV in Figs. 2 and 3. The entries in this table contain four values of  $\chi^2$ , which up-downwards are in the order I-IV. The error bars in  $\lambda$  and  $R$  are reduced from their present values to one tenth of them in steps  $1/N$ ,  $N = 1, 2, \dots, 10$ . Each one of the  $\lambda$  values corresponds to new physics, as is indicated by the small ellipses in Figs. 2 and 3. In Table 3 we can see how the resolution increases as the error bars in  $\lambda$  and  $R$  decreased.

To clearly resolve I and II it is quite sufficient to cut  $\sigma_R$  and  $\sigma_\lambda$  simultaneously to a little over one-half their current values. To resolve point IV requires that

$\sigma_R$  and  $\sigma_\lambda$  be simultaneously cut to around one sixth. To resolve the overall average of  $\lambda$  at III requires more effort, because of its closeness to the SMR. However, Fig. 3 shows it falls in the NPR. Also, one can see in this table that reducing  $\sigma_R$  alone is of little use in detecting new physics. While reducing  $\sigma_\lambda$  alone helps in cases I and II, but is useless in cases III and IV.

**Summary and discussion.** In this paper we have substantially improved the predictions of the SM for  $n\beta d$  observables, as can be appreciated by comparing Fig. 1 with Figs. 2 and 3. Our analysis has several implications. First, it allows to clearly and also easily appreciate recent precision measurements,  $\lambda LYB$  and  $\lambda_R$ . In Fig. 1 they show some indication in favor of new physics, while in Figs. 2 and 3 each one is clearly resolved past the 90% C.L. in favor of the latter. Of course, we still have to wait for a consistent average to be determined in the future. Second, our current inability to compute  $\lambda$  and  $R$  with the SM is not a real obstacle to detect new physics in  $n\beta d$ . Ideally, the SM predictions should be a point in the  $(\lambda, R)$ -plane. Instead, with  $\lambda$  and  $V_{ud}$  remaining as free parameters, the predictions become still ideally a line in this plane. Thus, it is still possible to resolve this line from new physics contributions. Third, the real limitations for this enterprise come from the width of the band around this ideal line. As we have seen, there are only two important ingredients in this width. One is the  $10^{-4}$  theoretical uncertainty in  $R$  and the other one is the error bars on  $V_{us}$ . The first one turns out to be not important. It forces us to stop at the band of Fig. 2. However, looking at Fig. 3, which assumes that this theoretical error has been reduced to zero, we learn that error bars of  $V_{us}$  are the real limitation for  $n\beta d$  to detect new physics. In the light of this discussion, we can understand better where future efforts should be directed. On the theoretical side, they should be directed towards reducing the theoretical uncertainties in  $R$  and in the determination of  $V_{us}$ . On the experimental side, our analysis makes it clear (see Table 3) that precision measurements must simultaneously reduce the error bars on  $R$  and  $\lambda$ . Improving measurements in only one of them is useless. The precision measurements of the other two angular coefficients  $\alpha_{e\nu}$  and  $\alpha_\nu$ , lead to the same bands of Figs. 2 and 3. In this sense they are no longer needed. However, if new physics is indeed detected in  $n\beta d$ , they will be very useful in delucidating what kind of new physics it would be. Finally, it is clear that the determination of  $V_{us}$  must be greatly improved, because it represents the real limitation for  $n\beta d$  to detect new physics.

**Acknowledgments.** The authors are grateful to CONACyT (México) for partial support.

Table 1

Ranges for  $\lambda$  at fixed values of  $R$ , in the three cases for the size of  $\sigma_\lambda$  and  $\sigma_R$  discussed in the text. For completeness, we also include the range for  $V_{ud}$ .  $\chi_0^2$  is the minimum of  $\chi^2$  and  $\lambda_0$  is the corresponding  $\lambda$ .

$R_0$	$\chi_0^2$	$\lambda_0$	b o u n d s o n $\lambda$		b o u n d s o n $V_{ud}$ 90% C.L.
			90% C.L.	95% C.L.	
1.13209	0.71	1.26988	(1.26581, 1.27464)	(1.26471, 1.27574)	(0.97832, 0.97270)
	0.75	1.26988	(1.26911, 1.27072)	(1.26883, 1.27103)	(0.97621, 0.97519)
	0.75	1.26990	(1.26952, 1.27041)	(1.26940, 1.27060)	(0.97539, 0.97597)
1.13099	0.65	1.26913	(1.26503, 1.27386)	(1.26393, 1.27496)	(0.97834, 0.97272)
	0.71	1.26913	(1.26835, 1.26997)	(1.26807, 1.27029)	(0.97622, 0.97519)
	0.69	1.26915	(1.26877, 1.26966)	(1.26865, 1.26985)	(0.97539, 0.97597)
1.12989	0.61	1.26839	(1.26424, 1.27308)	(1.26314, 1.27418)	(0.97837, 0.97274)
	0.67	1.26839	(1.26761, 1.26922)	(1.26734, 1.26953)	(0.97622, 0.97519)
	0.64	1.26840	(1.26802, 1.26891)	(1.26790, 1.26910)	(0.97539, 0.97597)
1.12879	0.56	1.26763	(1.26345, 1.27231)	(1.26235, 1.27341)	(0.97840, 0.97276)
	0.64	1.26763	(1.26687, 1.26846)	(1.26659, 1.26876)	(0.97622, 0.97520)
	0.59	1.26765	(1.26727, 1.26816)	(1.26715, 1.26835)	(0.97539, 0.97597)
1.12769	0.54	1.26689	(1.26268, 1.27154)	(1.26158, 1.27264)	(0.97842, 0.97277)
	0.60	1.26689	(1.26611, 1.26770)	(1.26582, 1.26801)	(0.97622, 0.97521)
	0.56	1.26689	(1.26651, 1.26741)	(1.26639, 1.26760)	(0.97539, 0.97597)
1.12659	0.52	1.26614	(1.26189, 1.27076)	(1.26079, 1.27186)	(0.97845, 0.97279)
	0.58	1.26614	(1.26536, 1.26695)	(1.26508, 1.26725)	(0.97623, 0.97521)
	0.52	1.26614	(1.26576, 1.26666)	(1.26564, 1.26685)	(0.97539, 0.97597)
1.12549	0.50	1.26539	(1.26110, 1.26998)	(1.26001, 1.27108)	(0.97848, 0.97281)
	0.56	1.26539	(1.26461, 1.26620)	(1.26433, 1.26652)	(0.97623, 0.97521)
	0.50	1.26539	(1.26501, 1.26591)	(1.26489, 1.26610)	(0.97539, 0.97597)

## References

- [1] H. Abele *et al*, Phys. Rev. Lett. **88** (2002) 211801, and references therein.
- [2] A. García, J.L. García-Luna, G. López Castro, Phys. Lett. **B500**, 66 (2001).
- [3] D.H. Wilkinson, Nucl. Instrum. Methods **A335**, (1993) 172, 182, 201 and references therein.
- [4] D. E. Groom, *et al*, Particle Data Group, Eur. Phys. J. **C15**, (2000) 1.
- [5] P. Liaud *et al*, Nucl. Phys. **A612**, (1997) 53.
- [6] P. Bopp *et al*, Phys. Rev. Lett. **56**, (1986) 919.
- [7] B. Yerozolimsky *et al*, Phys. Lett. **B412**, (1997) 240.
- [8] J. Reich *et al*, *V Int. Seminar on Interaction of Neutrons with Nuclei*, Dubna 1997.
- [9] D.H. Wilkinson, Z. Phys. **A348**, (1994) 129.

Table 2

Values of  $\chi^2$  at sample points in the  $(\lambda, R)$  plane for current  $\sigma_\lambda$  and  $\sigma_R$  (upper entries) and for one tenth of their current values (lower entries).

$R \setminus \lambda$	1.2552	1.2576	1.2600	1.2624	1.2648	1.2672	1.2696	1.2720	1.2744
1.13209	33.7 3352	23.7 2353	15.7 1440	9.2 805	4.7 354	1.9 87	0.8 1.1	1.3 32	3.4 230
1.13099	30.4 2924	21.0 1983	13.4 1224	7.6 647	3.6 253	1.3 41	0.7 0.8	1.7 74	4.4 328
1.12989	27.3 2613	18.4 1728	11.4 1026	6.2 506	2.7 168	0.9 12	0.8 5	2.3 133	5.6 443
1.12879	24.3 2320	16.0 1491	9.5 845	4.9 381	1.9 100	0.7 1.2	1.0 24	3.1 208	6.8 675
1.12769	21.5 2044	13.8 1272	7.8 682	3.8 275	1.3 51	0.6 0.6	1.5 62	4.0 302	8.2 725
1.12659	18.9 1784	11.7 1069	6.4 536	2.8 185	0.9 17	0.6 2.4	2.0 117	5.1 414	9.9 893
1.12549	16.4 1543	9.9 884	5.1 407	2.0 114	0.6 2.1	0.9 18	2.8 190	6.3 543	11.7 1079

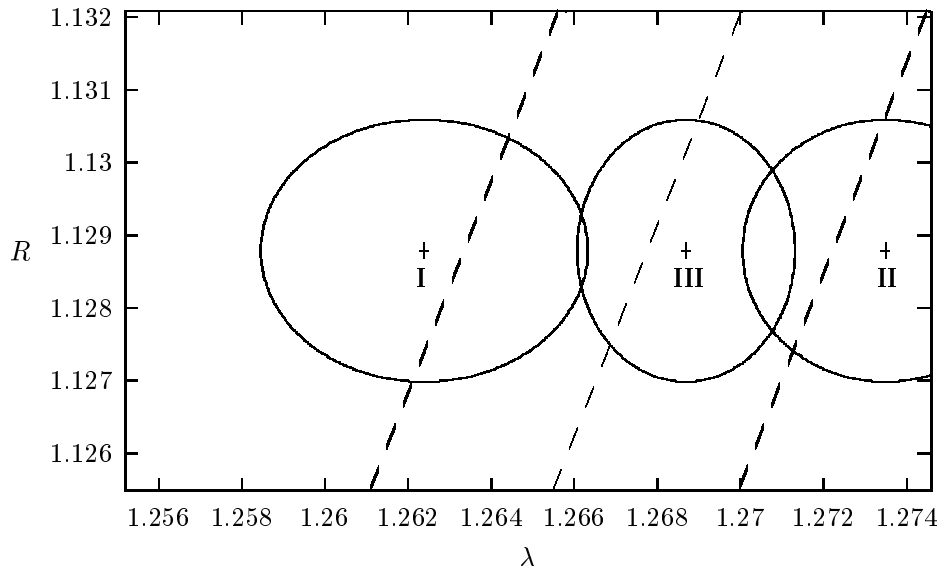


Fig. 1. The SMR, at current values of  $\sigma_\lambda$  and  $\sigma_R$ , is the band within the dotted lines. See text for other explanations.

Table 3

Increase of  $\chi^2$  as  $\sigma_\lambda$  and  $\sigma_R$  are reduced as  $1/N$ ,  $N = 1, 2, \dots, 10$ , at the points I–IV of figures 2 and 3. The up-downwards order is also I–IV.

$R \setminus \lambda$	$\sigma_\lambda/1$	$\sigma_\lambda/2$	$\sigma_\lambda/3$	$\sigma_\lambda/4$	$\sigma_\lambda/5$	$\sigma_\lambda/6$	$\sigma_\lambda/7$	$\sigma_\lambda/8$	$\sigma_\lambda/9$	$\sigma_\lambda/10$
$\sigma_R/1$	4.8	13.1	21.1	27.3	31.6	34.6	36.7	38.5	39.3	40.1
	7.4	20.2	31.5	39.3	44.2	47.6	50.0	52.0	52.9	53.8
	0.8	1.0	1.1	1.1	1.2	1.2	1.2	1.2	1.2	1.2
	1.2	2.3	3.1	3.8	4.3	4.6	4.8	5.0	5.1	5.2
$\sigma_R/2$	5.1	16.3	31.9	49.3	66.2	81.5	94.9	106	116	123
	8.0	26.6	51.2	77.0	101	121	139	152	164	173
	0.8	1.1	1.2	1.3	1.5	1.5	1.6	1.6	1.7	1.7
	1.2	2.6	4.2	5.9	7.7	9.4	10.8	12.0	13.1	14.0
$\sigma_R/3$	5.2	17.1	35.3	58.1	83.4	109	135	160	182	203
	8.1	28.1	58.2	94.5	133	172	209	242	272	298
	0.8	1.1	1.3	1.5	1.6	1.7	2.0	2.1	2.2	2.3
	1.3	2.6	4.5	6.8	9.4	12.1	14.8	17.3	19.8	22.0
$\sigma_R/4$	5.2	17.5	36.7	62.5	91.8	125	159	194	228	262
	8.1	28.8	61.2	103	150	202	254	305	354	400
	0.8	1.1	1.3	1.5	1.7	1.9	2.1	2.3	2.5	2.6
	1.3	2.7	4.7	7.1	10.1	13.5	17.0	20.6	24.9	27.8
$\sigma_R/5$	5.2	17.6	37.7	63.9	96.2	133	173	215	259	303
	8.1	29.1	62.7	107	160	219	282	347	412	476
	0.8	1.1	1.3	1.5	1.8	2.0	2.3	2.6	2.8	3.1
	1.3	2.7	4.8	7.5	10.8	14.6	18.3	22.7	27.8	31.7
$\sigma_R/6$	5.2	17.6	38.0	65.1	98.8	138	182	230	279	330
	8.1	29.3	63.5	109	166	230	300	375	452	530
	0.8	1.1	1.3	1.5	1.8	2.1	2.4	2.8	3.1	3.4
	1.3	2.7	4.7	7.6	10.8	14.7	19.2	24.6	29.8	34.3
$\sigma_R/7$	5.3	17.7	38.3	65.8	101	141	189	238	293	350
	8.1	29.4	64.0	111	169	240	312	394	480	569
	0.8	1.1	1.3	1.6	1.9	2.2	2.5	2.9	3.3	3.7
	1.3	2.7	7.7	11.2	11.2	15.0	19.7	25.4	30.3	36.1
$\sigma_R/8$	5.3	17.7	38.4	66.2	102	144	192	245	302	364
	8.1	29.4	64.4	112	172	242	321	408	501	598
	0.8	1.1	1.3	1.6	1.9	2.2	2.6	3.0	3.4	3.9
	1.3	2.7	4.7	7.7	11.3	15.2	20.0	25.4	32.0	37.4
$\sigma_R/9$	5.3	17.7	38.5	66.6	102	145	194	249	309	374
	8.1	29.5	64.6	113	173	245	327	418	516	620
	0.8	1.1	1.3	1.6	1.9	2.3	2.7	3.1	3.6	4.0
	1.3	2.7	4.7	7.7	11.1	15.4	20.3	25.8	31.9	39.3
$\sigma_R/10$	5.2	17.8	38.3	66.8	103	146	196	253	315	381
	8.1	29.5	64.8	113	175	248	332	425	527	636
	0.8	1.1	1.3	1.6	1.9	2.3	2.7	3.2	3.6	4.2
	1.3	2.7	4.8	7.7	11.2	15.5	20.5	26.1	33.2	39.1

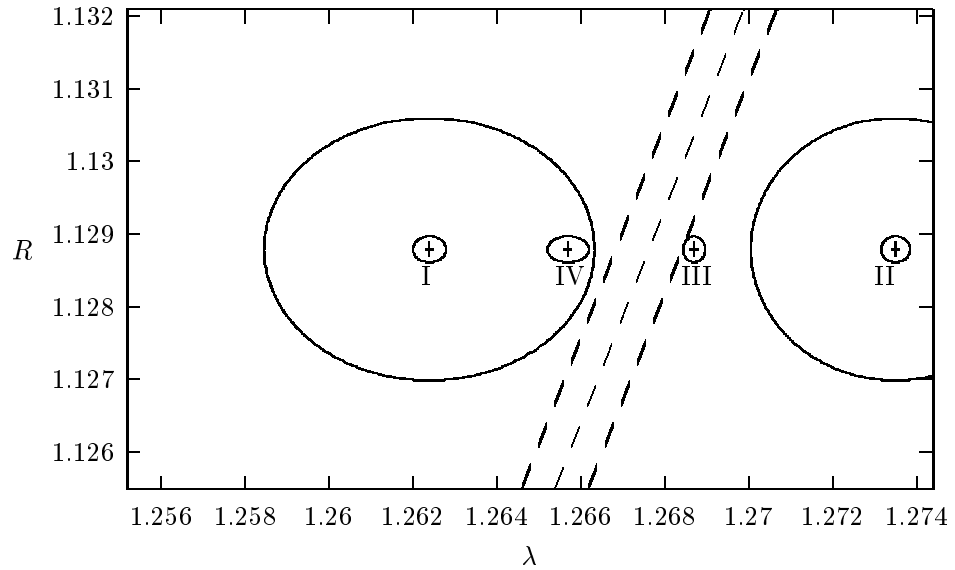


Fig. 2. The SMR, at one tenth of the current values of  $\sigma_\lambda$  and  $\sigma_R$ , is the band within the dotted lines. See text for other explanations.

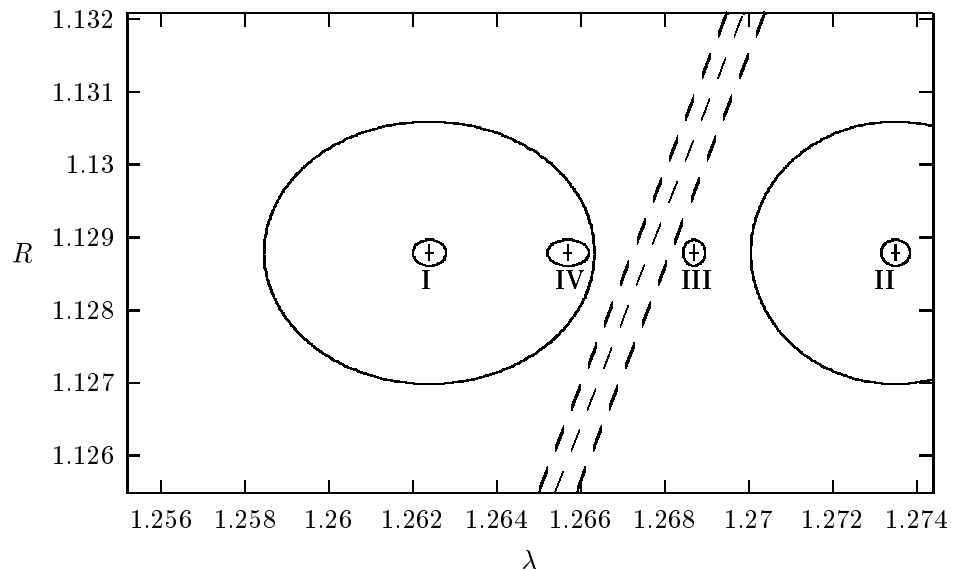


Fig. 3. The SMR, at one thousandth of the current values of  $\sigma_\lambda$  and  $\sigma_R$ , is the band with the dotted lines. See text for other explanations.